THE JOURNAL OF BIOLOGICAL CHEMISTRY VOL. 283, NO. 24, pp. 16906–16914, June 13, 2008
Printed in the U.S.A.

The Parkinson Disease-associated Leucine-rich Repeat Kinase 2 (LRRK2) Is a Dimer That Undergoes Intramolecular Autophosphorylation*[S]

Received for publication, October 22, 2007, and in revised form, April 3, 2008 Published, JBC Papers in Press, April 8, 2008, DOI 10.1074/jbc.M708718200

Elisa Greggio[‡1], Ibardo Zambrano[‡], Alice Kaganovich[‡], Alexandra Beilina[‡], Jean-Marc Taymans[§2], Veronique Daniëls[§3], Patrick Lewis[‡4], Shushant Jain[‡5], Jinhui Ding[¶], Ali Syed[‡], Kelly J. Thomas[‡], Veerle Baekelandt[§], and Mark R. Cookson[‡]

From the [‡]Cell Biology and Gene Expression Unit and the [¶]Bioinformatics Facility, Laboratory of Neurogenetics, NIA, National Institutes of Health, Bethesda Maryland 20892 and the [§]Laboratory for Neurobiology and Gene Therapy, Division of Molecular Medicine, Department of Molecular and Cellular Medicine, Katholieke Universiteit Leuven, 3000 Leuven, Belgium

Mutations in leucine-rich repeat kinase 2 (LRRK2) are a common cause of familial and apparently sporadic Parkinson disease. LRRK2 is a multidomain protein kinase with autophosphorylation activity. It has previously been shown that the kinase activity of LRRK2 is required for neuronal toxicity, suggesting that understanding the mechanism of kinase activation and regulation may be important for the development of specific kinase inhibitors for Parkinson disease treatment. Here, we show that LRRK2 predominantly exists as a dimer under native conditions, a state that appears to be stabilized by multiple domain-domain interactions. Furthermore, an intact C terminus, but not N terminus, is required for autophosphorylation activity. We identify two residues in the activation loop that contribute to the regulation of LRRK2 autophosphorylation. Finally, we demonstrate that LRRK2 undergoes intramolecular autophosphorylation. Together, these results provide insight into the mechanism and regulation of LRRK2 kinase activity.

Mutations in leucine-rich repeat kinase 2 *(LRRK2)*[6] are the single most common genetic cause of Parkinson disease (PD) (1, 2), accounting for 1–40% of all PD cases depending on the population studied (3–5). All mutations reported to date are inherited in a dominant fashion, albeit at reduced penetrance for some mutations (6). The phenotype of affected individuals is of clinical PD with variable pathology at autopsy (2, 7, 8).

The LRRK2 protein is large and complex, containing two enzymatic domains as well as several potential protein-protein interaction motifs. The various mutations are scattered throughout the protein with some evidence of clustering in the two enzymatic domains, which have kinase and GTPase activity, respectively (9–14). For example, the most common mutation (G2019S) is in the kinase domain, and there is a mutation at the adjacent residue, I2020T, that is the cause of PD in the family originally shown to segregate with the locus on chromosome 12 (8, 15). There are several mutations in the GTPase domain, including three at residue Arg-1441 (R1441C/R1441G/R1441H) and other mutations in the intervening sequences between GTPase and kinase domains.

We, and others, have shown that LRRK2 kinase activity is required for toxicity, at least in cell culture models (10, 16). An unresolved question is whether mutations consistently affect enzyme activity as published data on this are conflicting. The common G2019S mutation has consistently been shown to increase kinase activity by 2–3-fold (10, 14, 17, 18). Glycine 2019 is located at the Mg^{2+}-binding motif at the N-terminal end of the activation loop, a region of the kinase that is critical in the control of kinase activity. The effects of I2020T have been less clear, with both increases and decreases in kinase activity reported in different studies (9, 17, 19). Similarly varied impacts have been reported for mutations outside the kinase domain. LRRK2 and the related kinase LRRK1 can both bind GTP, and non-hydrolyzable GTP analogues increase kinase activity (11, 20–22). Mutations such as R1441C or R1441G decrease GTPase activity (11–13), thus potentially increasing the length of time that the molecule has increased kinase activity following GTP binding.

Part of the difficulty with assessing how mutations affect kinase activity is that our knowledge of how these large complex kinases work is, at best, nascent. A previous study using fragments of LRRK2 expressed as recombinant proteins in *Escherichia coli* has shown that LRRK2 can phosphorylate itself efficiently and that there are key residues within the activation loop

* This work was supported, in whole or in part, by the National Institutes of Health Intramural Research Program of the NIA. The costs of publication of this article were defrayed in part by the payment of page charges. This article must therefore be hereby marked "*advertisement*" in accordance with 18 U.S.C. Section 1734 solely to indicate this fact.

[S] The on-line version of this article (available at http://www.jbc.org) contains supplemental text and a supplemental figure.

[1] To whom correspondence should be addressed: Laboratory of Neurogenetics, NIA, National Institutes of Health, Bldg. 35, Rm. 1A1012, MSC 3707, 35 Convent Dr., Bethesda, MD 20982-3707. Tel.: 301-451-3831; Fax: 301-451-7295; E-mail: greggio@mail.nih.gov.

[2] A postdoctoral fellow of the Flemish Fund for Scientific Research (FWO Vlaanderen).

[3] A research assistant of the Flemish Fund for Scientific Research (FWO Vlaanderen).

[4] Present address: Dept. of Molecular Neuroscience and Rita Lila Weston Laboratories, Institute of Neurology, Queen Square, London WC1N 3BG UK.

[5] Present address: Dept. of Clinical Genetics, Section of Medical Genomics, Vrije Universiteit Medical Center, van der Boechorststraat 7, 1081 BT Amsterdam, Netherlands.

[6] The abbreviations used are: LRRK2, leucine-rich repeat kinase 2; PD, Parkinson disease; COR, C-terminal of ROC; GFP, green fluorescent protein; GST, glutathione *S*-transferase; PDB, Protein Data Bank; FPLC, fast protein liquid chromatography; ROC, Ras of complex proteins; MBP, myelin basic protein; Bis-Tris, 2-(bis(2-hydroxyethyl)amino)-2-(hydroxymethyl)propane-1,3-diol; KD, kinase dead; WT, wild type.

of the kinase that control activity (18). In the present study, we have examined the autophosphorylation activity of the intact, full-length LRRK2 protein expressed in mammalian cells. We show that autophosphorylation is affected by Ser/Thr mutations in the activation loop of LRRK2. However, and in contrast to fragments expressed in *E. coli*, our data support the idea that full-length LRRK2 undergoes *cis* rather than *trans* autophosphorylation. We suggest that these differences are due to the complex topology of LRRK2, which results in the formation of dimeric species *in vivo*.

EXPERIMENTAL PROCEDURES

Constructs and Cell Culture—Full-length LRRK2 was cloned to generate N-terminal 2x-Myc or GFP and C-terminal V5-His tagged proteins as described previously (10, 21). Mutagenesis to generate artificial activation loop mutations was performed using the QuikChange II site-direct mutagenesis (Stratagene, La Jolla, CA). Truncated forms of LRRK2 were amplified from full-length cDNA using *Pfu* polymerase (Stratagene), cloned into pCR8GW/TOPO (Invitrogen), and subcloned into 2x-Myc destination vectors (21). Roc and WD40 domains were amplified and cloned in fusion with GFP in the pEGFP-C1 plasmid via the BglII and KpnI sites of the multiple cloning site. GFP was excised from these constructs via NheI and BspEI digestion and replaced by a short adaptor containing the 3x-FLAG tag (for Roc and WD40) or the 3x-Myc tag (for Roc). All plasmids were fully sequenced. Constructs were transfected in HEK293FT or COS7 cells using FuGENE 6 (Roche Applied Science). Cells were harvested 48 h after transfection. Lymphoblastoid cell lines were used for endogenous LRRK2 as these cells have been shown previously to express high levels of the protein (23).

Yeast Two-hybrid Screening—Yeast two-hybrid strain AH109 harboring the HIS3, ADE2, and lacZ reporters were transformed with a portion of LRRK2 (amino acids 1270–1435) fused to the Gal4 DNA-binding domain. This construct was determined to be negative in self-activation of all selection markers by co-transformation with empty vectors. Yeast harboring the LRRK2-DNA-binding domain construct were mated with yeast containing a human brain cDNA library fused to the activation domain (premade Matchmaker pretransformed cDNA libraries, Clontech). Mated yeast were grown on $Trp^-/Leu^-/His^-/Ade^-$ plates for 4 weeks to assay for interaction. Positive clones were grown, and the prey inserts were isolated and sequenced.

GST Pulldowns—HEK293FT cells were transfected with GFP-tagged full-length LRRK2 or Myc-tagged truncated LRRK2 and lysed in 20 mM Tris-HCl, pH 7.5, 150 mM NaCl, 1 mM Na_2EDTA, 1 mM EGTA, 1% Triton, 2.5 mM sodium pyrophosphate, 1 mM β-glycerophosphate, 1 mM Na_3VO_4, 1 μg/ml leupeptin, protease inhibitor mixture (Roche Applied Science). Glutathione-Sepharose beads with purified recombinant proteins were incubated with total cell lysates for 2 h at 4 °C. After four washes (phosphate-buffered saline, 150 mM NaCl, 1% Triton X-100, and protease inhibitors), copurified proteins were analyzed by immunoblot with anti-GFP or anti-Myc antibody (Roche Applied Science).

Co-immunoprecipitation—HEK293FT cells were co-transfected with GFP-tagged and V5-tagged full-length LRRK2 or 3x-Myc-tagged Roc-LRRK2 and 3x-FLAG-tagged Roc or WD40. After 48 h, cells were lysed and incubated with anti-GFP antibody or anti-Myc-agarose beads at 4 °C (Invitrogen). After four washes, immunoprecipitates were analyzed by Western blotting with anti-V5 antibodies (Invitrogen), anti-GFP antibodies (Roche Applied Science), anti-Myc antibodies (9e10, Roche Applied Science), or anti-FLAG antibodies (M2, Sigma).

Size Exclusion Chromatography and Native PAGE—Size exclusion chromatography was carried out at 4 °C using the Amersham Biosciences Akta-FPLC system. Transiently transfected COS7 cells were lysed on ice for 30 min (0.1% Triton X-100 in 1× phosphate-buffered saline supplemented with protease inhibitors), and cleared lysate (0.25 ml) was injected for FPLC. Gel filtration was a Superdex 200 HR 10/30 column (Amersham Biosciences) equilibrated with lysis buffer at 0.4 ml/min. Column void volume was 7.8 ml, and elution volumes of standards (Amersham Biosciences and Sigma) were 10.80 ml for ferritin (440 kDa), 12.3 ml for catalase (232 kDa), 12.8 ml for aldolase (158 kDa), 13.8 ml for transferrin (80 kDa), and 14.8 ml for ovalbumin (43 kDa). Fractions (0.25 ml) were analyzed by SDS-PAGE and immunoblotting using monoclonal anti-Myc antibody (Roche Applied Science) or a polyclonal anti-peptide antibody raised against residues 2079–2100 of human LRRK2 (Sigma). For native PAGE, 30 μg of total cell lysates transfected with Myc-LRRK2 were loaded into 3–12% Bis-Tris gels (Invitrogen). Gels were transferred onto Immobilon-P membranes (Millipore), and membranes were probed with anti-Myc antibody (9e10, Roche Applied Science) or rabbit anti-LRRK2.

In Vitro Kinase Assays—Myc-tagged LRRK2 proteins immunoprecipitated from HEK293FT were incubated on the agarose beads with 40 μl of kinase buffer (25 mM Tris-HCl (pH 7.5), 5 mM β-glycerophosphate, 2 mM dithiothreitol, 0.1 mM Na_3VO_4, 10 mM $MgCl_2$) containing 3 μCi of [^{32}P]ATP (3000 Ci/mmol; PerkinElmer Life Sciences) per reaction for 30 min at 30 °C. Reactions were terminated by adding Laemmli buffer, loaded onto precast Tris-HCl gel 4–20% or 5% (Bio-Rad) and transferred onto Immobilon-P membranes (Millipore). Incorporated [^{32}P]ATP was detected by autoradiography, and the same membranes were probed with anti-Myc antibody for total protein loading.

Structural Modeling—The structural model of the kinase domain of LRRK2 was constructed using kinase TβR-I (PDB entry 1B6C) as a template. Because more than one template was available in the Protein Data Bank, structure-based profile-energy score (24) was used to guide template selection. PDB entry 1B6C has the best structure-based profile-energy score among the other serine/threonine kinase structures, so it was chosen as the model template. Sequence alignment between LRRK2 kinase domain and TβR-I kinase was performed using CLUSTALX (25), and all alignments were manually adjusted to keep the overall secondary structures. The Jackal package (26) was applied in model building, loop prediction, and refinement. The final model underwent several rounds of energy minimization to solve the clashes between residues.

Statistical Analysis—Statistical significance was assessed using one-way analysis of variance followed by Tukey's multiple

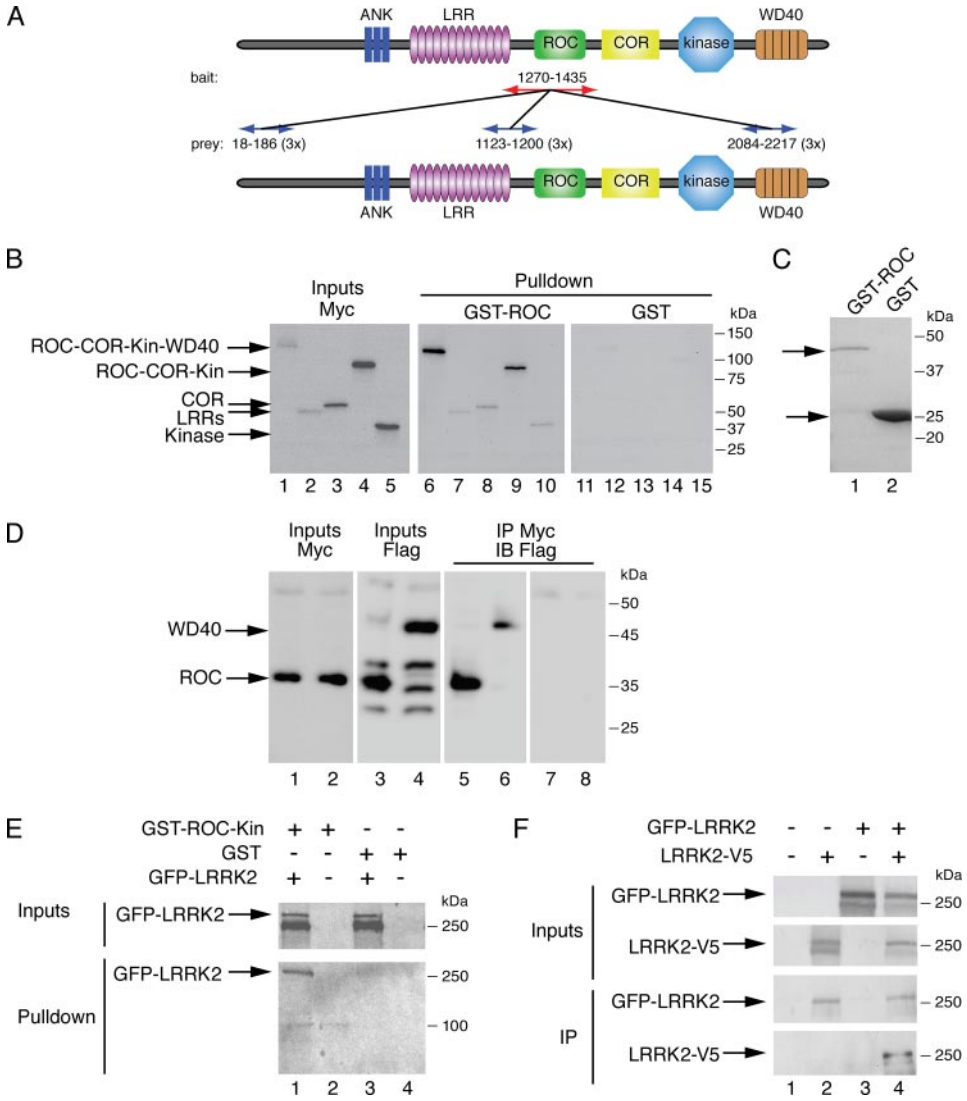

FIGURE 1. **LRRK2 self-interacts.** *A*, schematic of the yeast two-hybrid results obtained using a central part of LRRK2 as bait (*upper illustration*). Interacting fragments of LRRK2 are shown by *double-headed arrows* (*lower illustration*). *ANK* = ankyrin domain. *B*, mapping interactions of the ROC domain against Myc-LRRK2 fragments expressed in 293FT cells. The *left panel* shows inputs, the *central panel* represents GST-ROC pulldowns, and the *right panel* represents GST pulldowns. Membranes were probed with Myc (9e10) antibody. *Kin*, kinase. *C*, Coomassie Blue staining of GST and GST-ROC proteins used for pulldown experiments. *D*, mapping interactions of the ROC domain by co-immunoprecipitation (*IP*). Myc-ROC or vector control plasmids were co-expressed together with FLAG-ROC and FLAG-WD40 in 293FT cells, and proteins were co-immunoprecipitated. The *left panels* show inputs (Myc-ROC on *lanes 1–2*; FLAG-ROC and FLAG-WD40 on *lanes 3–4*), and the *right panels* show co-immunoprecipitations by Myc-ROC (*lanes 5–6*) or by vector control (*lanes 7–8*). Membranes were probed with anti-Myc (9e10; *lanes 1–2*) or anti-FLAG (M2; *lanes 3–8*) antibodies. *IB*, immunoblot. *E*, GST pulldowns of ROC-COR-kinase with GFP-full-length LRRK2 expressed in 293FT cells. Recombinant ROC-COR-kinase was expressed in *E. coli* as GST fusion protein and purified by glutathione affinity chromatography. The *upper panel* indicates inputs, and the *lower panel* indicates pulldowns. Blots were probed with anti-GFP monoclonal antibody. *F*, full-length LRRK2 interaction. Co-immunoprecipitation of GFP-LRRK2 and LRRK2-V5 overexpressed in 293FT cells. Immunoprecipitations were performed using anti-GFP antibodies. Inputs (*upper panels*) and immunoprecipitates (*lower panels*) were probed with either GFP or V5 antibodies. The *arrows* indicate position of LRRK2, and the *markers* on the *right* of the blots are in kilodaltons.

ROC (Ras of complex proteins) domain and part of the leucine-rich repeats (LRRs) domain (amino acids 1270–1435) and identified several clones encoding three distinct portions of LRRK2. These were part of (i) the non-annotated N-terminal region (18–186), (ii) the LRRs and a region just before the ROC domain (1123–1200), and (iii) the C-terminal WD40 domain (2084–2217; Fig. 1*A*). These results suggested that LRRK2 exhibits self-interaction through different domains.

To confirm the initial yeast two-hybrid results, we used GST pulldowns and co-immunoprecipitation (Fig. 1, *B–D*) to precipitate Myc- or FLAG-tagged LRRK2 fragments from transfected cells. Using the GST-ROC domain, we could pull down the central portion of the LRRK2 molecule (ROC-COR-kinase domains; Fig. 1*B*, *lane 9*), consistent with predictions from the above screen. This interaction was strengthened by inclusion of the WD40 domain (Fig. 1*B*, *lane 6*), suggesting that this region also contributes to self-interaction. We also observed interaction between the ROC domain and the two adjacent regions COR and LRRs (Fig. 1*B*, *lanes 7* and *8*). The ability of ROC to pull down LRRs confirms the yeast two-hybrid findings, whereas the interaction with COR domain, which we have previously shown (28), likely suggests that these two contiguous domains physically interact. The kinase domain showed only a very weak interaction with ROC (Fig. 1*B*, *lane 10*). However, the N-terminal region of LRRK2 was not stable when expressed in mammalian cells or as recombinant fusion proteins (data not shown). Therefore, although our yeast two-hybrid data also support a self-association of LRRK2 that is mediated through the central ROC domain and the N terminus, we have not been able to formally assess whether this part of the protein is sufficient for interaction. GST alone did not pull down LRRK2 under the same conditions (Fig. 1*B*), even when an excess amount was added relative to the GST-ROC domain (Fig. 1*C*). Although we observed that the presence of WD40 domain strengthens the interaction with ROC in GST pulldowns (Fig. 1*B*), we confirmed this result by showing a direct interaction

comparison test. Differences were considered significant when $p < 0.05$.

RESULTS

LRRK2 Self-interacts—Dimerization is a common mechanism to regulate the activity of protein kinases (27). We performed a yeast two-hybrid screen for possible protein interactors of the central portion of LRRK2 encompassing mainly the

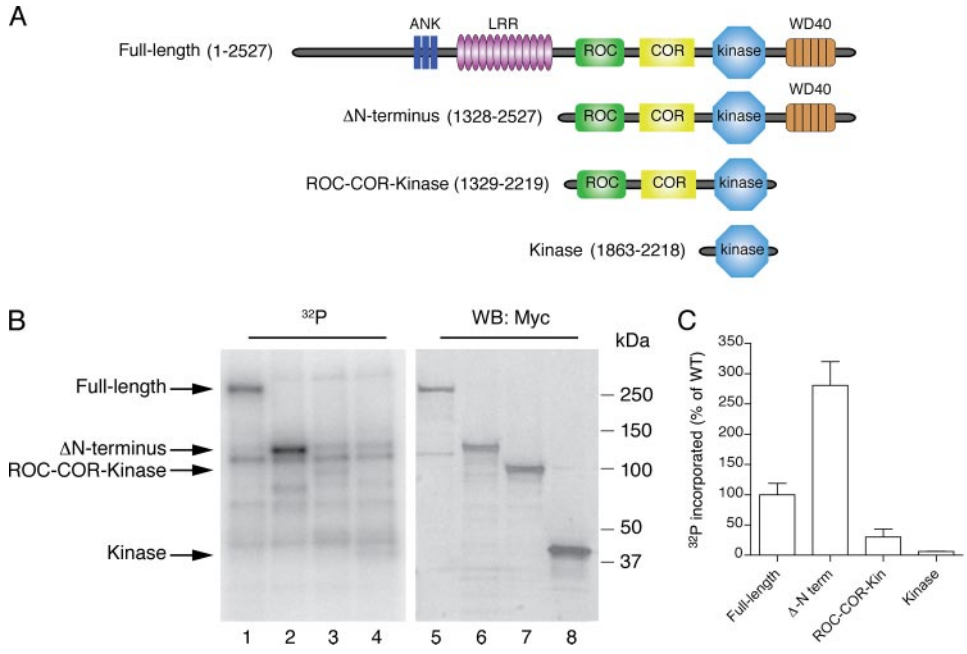

FIGURE 2. **Truncated forms of LRRK2 show decreased autophosphorylation.** *A*, schematic of deletion constructs analyzed for their ability to undergo autophosphorylation. *ANK* = ankyrin domain. *B*, the *left panel* represents autophosphorylation of immunoprecipitated proteins, and the *right panel* shows total protein loading by immunoblot with Myc (9e10) antibody. Full-length proteins (*lane 1*) exhibit autophosphorylation as expected; ΔN terminus (*lane 2*) displayed high levels of autophosphorylation; ROC-COR-kinase (*lane 3*) and kinase (*lane 4*) were incompetent to undergo autophosphorylation, although the amounts immunoprecipitated were comparable with active proteins (Western blot (*WB*) with anti-Myc, *right panel*, *lanes 5–8*). *C*, quantitation indicates that ΔN terminus (*ΔN term*; amino acids 1328–2527) incorporates approximately three times more ^{32}P than full-length. Both ROC-COR-kinase and kinase domains incorporated almost undetectable amounts of ^{32}P. All experiments were carried out in triplicate.

between Myc-tagged ROC and FLAG-tagged WD40 by co-immunoprecipitation (Fig. 1*D*, *lane 4*). We also successfully co-immunoprecipitated the ROC domain with itself (Fig. 1*D*, *lane 3*), supporting the yeast two-hybrid results and the crystal structure of dimeric ROC (PDB entry 2ZEJ (Ref. 28)).

To extend this, we pulled down full-length LRRK2 with a GST fusion protein that included the ROC, COR, and kinase domains (Fig. 1*E*). As above, GST alone gave no signal, and no signal was seen in non-transfected cells. We showed that two full-length LRRK2 molecules are also able to interact by co-immunoprecipitating N-terminal GFP-tagged and C-terminal V5-tagged proteins (Fig. 1*F*).

We next asked whether these interactions might contribute to the kinase activity of the full-length protein expressed in mammalian cells. Different truncation constructs containing a Myc tag (Fig. 2*A*) were expressed and immunoprecipitated from 293FT cells and subjected to an *in vitro* kinase assay. Full-length LRRK2 and a deletion construct lacking the N terminus region and the LRRs (amino acids 1328–2527) displayed autophosphorylation activity (Fig. 2*B*). Interestingly, proteins lacking the N terminus incorporated approximately three times more ^{32}P when compared with full-length proteins (Fig. 2*C*). We also detected autophosphorylation using a construct that included the LRRs (amino acids 796–2527), but this fragment was unstable, and only a small amount of protein could be expressed and immunoprecipitated (data not shown). In contrast, the ROC-COR-kinase domain and the kinase domain alone expressed at high levels in 293FT, suggesting that they are intrinsically stable but had very low activity in autophosphorylation assays (Fig. 2, *B* and *C*). Together, these observations indicate that the C terminus WD40 domain is not only crucial for LRRK2 self-interaction but also crucial for autophosphorylation activity.

LRRK2 Is Predominantly a Dimer—Collectively, the previous results show that LRRK2 self-interacts and are consistent with a previous report using tandem affinity purification (9) but do not define the nature of the species formed (*i.e.* dimer, trimer, etc.). We therefore used two techniques that address the size of the native complex formed by LRRK2, namely blue native PAGE and size exclusion chromatography. In these experiments, we used two artificial mutant versions of LRRK2 that have decreased kinase activity relative to wild-type protein. The triple kinase dead (K1906A/D1994A/D2017A (10)) has a small residual activity when compared with wild type, whereas the GTP binding-deficient variant, K1347A (12), retains about 50% of the activity of wild-type when all three versions are assayed at the same time (Fig. 3*A*).

Blue native PAGE revealed that LRRK2 is mainly present in a complex with an estimated molecular weight consistent with a dimer (estimated size 550 kDa) (Fig. 3*B*). A smeared signal from the dimer up to 1.2 MDa was also seen, suggesting that LRRK2 is additionally present in larger complexes. Using gel filtration, we observed that the majority of transfected wild-type Myc-LRRK2 elutes as a complex of ~600 kDa, slightly larger than the size of a putative LRRK2 dimer (Fig. 3, *C* and *D*). Very little protein was found in the fraction around 250–300 kDa that would correspond to a monomeric form of LRRK2. At higher molecular masses, a smaller peak (~35% of the dimer peak) was observed at around 1.3 MDa in FPLC (Fig. 3*C*). All these experiments were performed in transfected COS7 cells, but we found similar results using HEK293FT cells (data not shown). Interestingly, the triple mutant kinase dead or K1347A versions tended not to be present in the dimer peaks but in the larger complexes using both techniques (Fig. 3, *B–D*), suggesting a slightly different propensity to form dimers for these two variants (see discussion).

Although the above results suggest that transfected protein is capable of forming both dimers and higher molecular weight species, it is possible that this is an artifact of high expression levels achieved in heterologous cell lines. To address this, we surveyed a number of human cell lines for endogenous levels of LRRK2 and found that lymphoblastoid cell lines expressed the most readily detectable signal (data not shown), which has also been reported by Melrose *et al.* (23). Using these cells, we per-

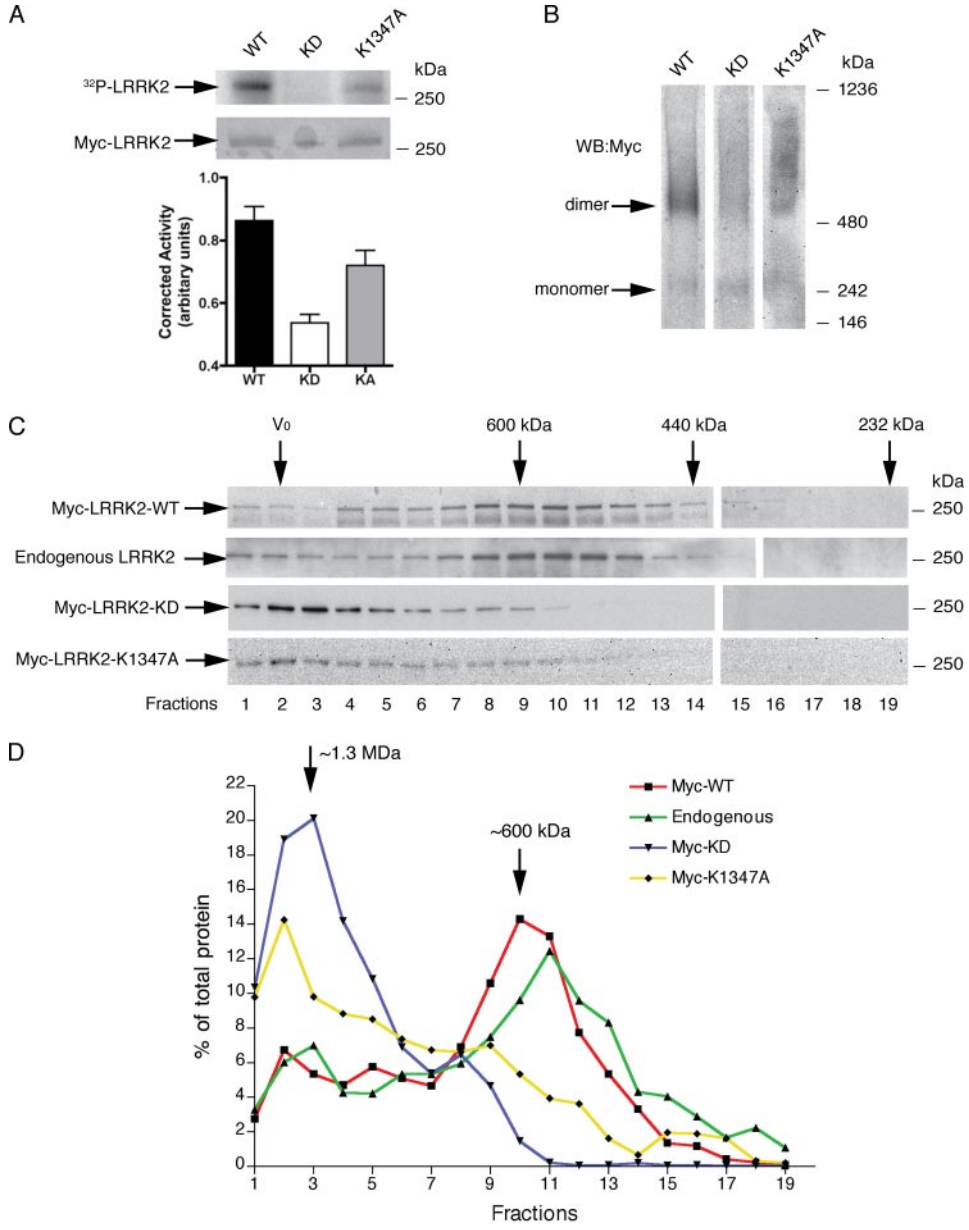

FIGURE 3. **Active LRRK2 forms dimers.** *A*, autophosphorylation activity of immunoprecipitated Myc-tagged wild-type, kinase dead (KD), and K1347A LRRK2. Blots are representative of $n = 3$ independent experiments, and corrected activity for total loading (with anti-Myc antibody) are shown in a bar graph. *B*, native PAGE reveals that Myc-tagged wild-type (WT)-LRRK2, but not KD, and that K1347A is mainly present in a complex (~550 kDa) around the dimer size. A faint band is detected at ~270 kDa, corresponding to monomeric LRRK2. *WB*, Western blot. *C*, representative Western blot of 0.25-ml gel filtration fractions of wild-type, KD, and K1347A LRRK2 cell lysates. The column void volume (V_0) and the standards ferritin (*440 kDa*) and catalase (*232 kDa*) are indicated. Blots were probed either with anti-Myc (9e10) or with rabbit anti-LRRK2. *D*, graph illustrates the elution profile of Myc-tagged wild-type LRRK2 plotted as the average percentage of protein in each fraction from four independent extracts. The total signal in each fraction measured by densitometry was divided by the total signal of the protein in all the fractions to determine the percentages shown in the graph. LRRK2 exists mainly as a ~600-kDa species. A portion of the protein is present in higher molecular weight complexes. *Markers* on the *right* of all blots are in kilodaltons.

formed FPLC and saw a ~600-kDa peak and a broad higher molecular weight complex for the endogenous protein, similar to Myc-tagged wild-type LRRK2 (Fig. 3, *C* and *D*).

Mutations at Ser-2032 and Thr-2035 Decrease LRRK2 Autophosphorylation Activity—For many protein kinases, dimerization is mediated by autophosphorylation of key residues in the activation loop, which includes the region between the conserved DFG/DYG and APE motifs (29). Often, phosphorylation of one or more residues in the activation loop allows the loop to change conformation, usually resulting in an increased affinity for substrate binding. We constructed a structural model of the kinase domain of LRRK2 using the serine/threonine kinase domain of TβR-I (PDB entry 1B6C) as a template (Fig. 4*A*). Since LRRK2 has been shown to be a serine-threonine kinase (19), we identified three residues that might be candidate sites for modification in the activation loop, Thr-2031, Ser-2032, and Thr-2035. We made alanine mutants at all three sites and glutamate mutants at Ser-2032 and Thr-2035 (see below). Using native PAGE, we observed that, in contrast with kinase inactive LRRK2, all Myc-LRRK2 activation loop variants showed the same electrophoretic pattern with the main signal around the dimeric complex (Fig. 4*B*), showing that these variants do not affect dimer formation. Furthermore, these variants were expressed at similar levels to the wild-type protein (Fig. 4, *C* and *D*) in contrast to the triple kinase dead or K1347A artificial mutations that were less stable (compare with Fig. 3*A*).

As shown in Fig. 4, *C*–*F*, mutation of Thr-2031 to alanine did not change the autophosphorylation levels of LRRK2 when compared with the wild-type proteins. However, S2032A exhibited lower autophosphorylation levels when compared with wild type, and T2035A had activity similar to kinase-dead LRRK2 (Fig. 4*E*). We also mutated Ser-2032 and Thr-2035 to glutamate to examine whether the activity could be rescued by mimicking the phosphate negative charge. We observed a partial rescue of autophosphorylation only in the case of S2032E (Fig. 4, *C* and *E*) but the same level of ^{32}P incorporation by T2035E when compared with the alanine variant (Fig. 4*C*, $p < 0.05$) (Fig. 4*E*). In terms of myelin basic protein (MBP) phosphorylation, we observed a significant reduction in ^{32}P incorporation only for LRRK2-kinase dead (Fig. 4*F*, $p < 0.05$), although we could still detect some background. The activation loop mutants showed a slight decrease in MBP phosphorylation, which, however, did not reach significance. Therefore,

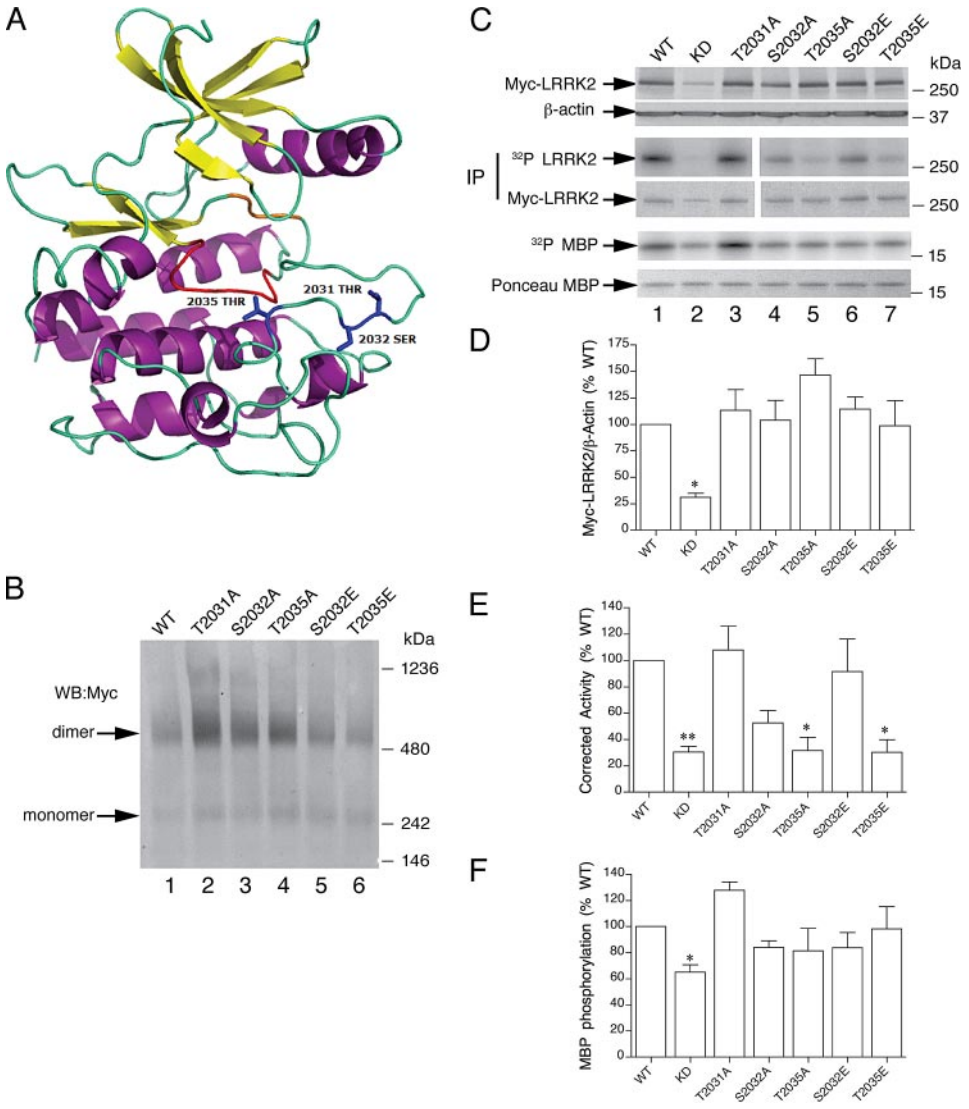

FIGURE 4. **Ser-2032 and Thr-2035 regulate LRRK2 autophosphorylation activity but are not sufficient to mediate dimerization.** *A*, the structural model of kinase domain of LRRK2 constructed using the serine/threonine kinase domain of TβR-I (PDB entry 1B6C) as a template highlights the position of potential regulatory sites Thr-2031, Ser-2032, and Thr-2035. The loop in *red* is the catalytic loop (it also chelates the secondary Mg^{2+} ion). The loop in *orange* contains the highly conserved ASP that chelates the primary activating Mg^{2+} ion. *B*, native PAGE followed by Western blots (*WB*) of the Myc-LRRK2 proteins where these sites are mutated to alanine or glutamate. All variants form dimers and a higher molecular weight smear with a minor band corresponding to monomeric LRRK2. *C*, WT, KD, and Ala/Glu mutants were cloned in fusion with an N terminus 2x-Myc tag and expressed in 293FT cells. Total lysates were blotted for Myc (9e10) and normalized with β-actin (*upper panels*). The same set of constructs was immunoprecipitated (*IP*) with anti-Myc polyclonal antibodies and subjected to *in vitro* kinase assays. Autophosphorylation activity is shown by autoradiography, and total proteins after immunoprecipitation are shown by Myc Western blot (*middle panels*). Activity against the generic Ser/Thr kinase substrate MBP was also assessed (*lower two panels*) using autoradiography, with MBP loading assessed using Ponceau staining. *Markers* on the *right* of the blots are in kilodaltons. *D–F*, quantitation indicates that and Thr-2035 and Ser-2032 mutations were fully stable (*D*) and had decreased autophosphorylation activity (*E*) but only minor effects on MBP phosphorylation (*F*). *D–F* were carried out in quadruplicate and analyzed by one-way analysis of variance with Tukey's multiple comparison test. *, $p < 0.05$; **, $p < 0.01$.

these two sites have a more readily detectable impact on autophosphorylation than phosphorylation of heterologous substrates.

LRRK2 Autophosphorylation Is an Intramolecular Process—Given the dimeric nature of LRRK2, we asked whether a given monomer within the complex phosphorylates itself (*cis*-phosphorylation) or the other constituent monomer (*trans*-phosphorylation). To investigate this mechanism, we used two electrophoretically distinct LRRK2 proteins, one a GFP-tagged kinase dead LRRK2 and one a Myc-tagged wild-type LRRK2, and analyzed them via 5% SDS-PAGE. We found that Myc-LRRK2 wild-type was not able to *trans*-phosphorylate GFP-LRRK2-kinase dead even using increasing concentration of Myc wild type up to ~1 μg (Fig. 5*A*). This observation suggests that autophosphorylation occurs *in cis*. To exclude the possibility that this result is limited only to the triple kinase dead, we checked whether GFP wild-type proteins were able to *trans*-phosphorylate other autophosphorylation-deficient variants of LRRK2 carrying a Myc tag. As shown in Fig. 4*B*, active GFP-LRRK2 was unable to phosphorylate Myc-kinase dead, which was expressed at lower levels than wild-type protein, but also S2032A, T2035A, and T2035E, which were expressed at similar levels (compared also with Fig. 4, *C* and *D*). We also analyzed the same set of Myc-tagged proteins using GFP-kinase dead with consistent results (Fig. 5*C*).

We further investigated whether LRRK2 activation loop alone could be a substrate for the full-length protein. LRRK2 activation loop (DYG . . . APE) was cloned in fusion with GST (supplemental Fig. 1*A*), expressed in *E. coli*, and purified by affinity chromatography using glutathione-Sepharose beads. Approximately 5 μg of either GST alone or the GST activation loop were used as substrates for Myc-LRRK2 wild-type and Myc-LRRK1 wild-type overexpressed and immunoprecipitated from 293FT cells. As shown in supplemental Fig. 1*B*, neither LRRK1 nor LRRK2 were able to phosphorylate the GST activation loop, further supporting the preference of LRRK2 to undergo intramolecular autophosphorylation. These results alone are not an unequivocal proof of *cis*-phosphorylation since activation loops may have highly constrained conformations within the protein, and it is possible that the GST activation loop does not have the proper confirmation. However, these data are at least consistent with the possibility that LRRK2 undergoes *cis*-autophosphorylation.

Taken together, these data indicate that LRRK2 monomers interact to form a dimer but the kinase domains autophospho-

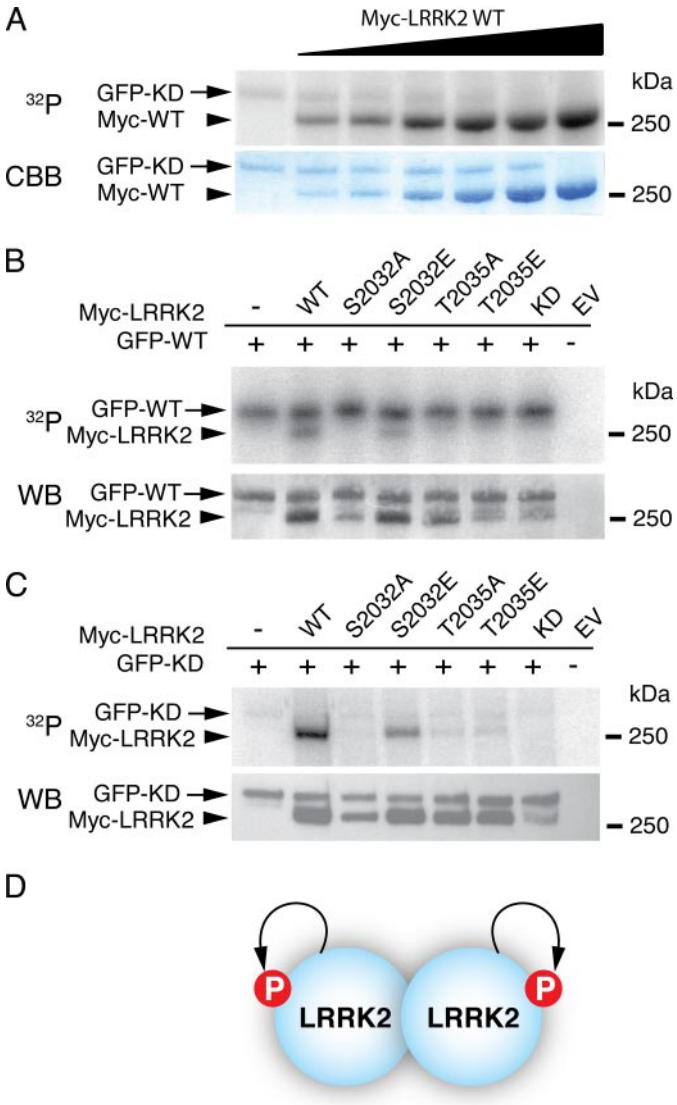

FIGURE 5. **Autophosphorylation of full-length LRRK2 is an intramolecular process.** *A*, *trans*-phosphorylation assays using GFP-KD as substrate and Myc-WT as active LRRK2. Proteins were purified by immunoprecipitation, and concentrations were estimated using bovine serum albumin standard on Coomassie Brilliant Blue (*CBB*). Constant amounts of GFP-KD (~100 ng) and increasing amounts of Myc-WT (from ~50 ng to ~1 μg) were loaded in 5% SDS-PAGE gels. Phosphorylation is shown by autoradiography (*upper panel*), and total protein loading is shown by Coomassie Brilliant Blue staining (*lower panel*). The experiment is representative of $n = 3$ replicates. *B*, *trans*-phosphorylation assays using Myc-LRRK2 WT, S2032A, S2032E, T2035A, T2035E, and KD and active GFP-WT. The *upper panel* represents autoradiograms, and the *lower panel* shows total protein loading by immunoblot (with monoclonal anti-GFP and Myc antibodies). *WB*, Western blot. *EV*, empty vector. *C*, *trans*-phosphorylation assays using the same set of Myc-tagged LRRK2 protein as *A* and GFP-KD as inactive substrate. As above, the *upper panel* represents autoradiograms, and the *lower panel* shows total protein loading by immunoblot. *D*, schematic showing that autophosphorylation (indicated by *circled P*) of dimeric LRRK2 is likely to be an intramolecular event.

rylate within the same monomer (Fig. 5*D*). Nonetheless, we cannot exclude the possibility that autophosphorylation occurs in a *trans*-intradimeric manner if the homodimers are tightly associated (see "Discussion").

DISCUSSION

In the present study, we investigated the size of the LRRK2 complex and its mechanism of autophosphorylation. We and others have previously shown that kinase activity is required for LRRK2 toxicity in neurons (10, 16), suggesting that further characterization of the mechanism of LRRK2 activity is critical to develop specific kinase inhibitors as a potential therapeutic strategy for PD. Here, we have shown that LRRK2 predominantly exists in a dimeric conformation *in vivo* with different points of interactions through each individual monomer. In a yeast two-hybrid experiment, we used the ROC domain as bait and found interactions with several regions of LRRK2, including a central portion (LRRs and a region before ROC), the WD40 domain, and the N terminus region. These observations, which we have validated by GST pulldown and co-immunoprecipitation experiments, suggest that the topology of dimeric LRRK2 is complex and that the interaction between the monomers is probably strong. We also confirmed the interaction between full-length LRRK2 proteins. These data are consistent with previous findings describing self-interaction of LRRK2 using a different technique, namely tandem affinity purification (9).

The presence of three predicted protein-protein interaction domains (ankyrin repeats, LRRs, and WD40) suggests that the LRRK2 complex is likely to include other proteins. We analyzed the size of the LRRK2 complex under native conditions using size exclusion chromatography and native PAGE. We found a strong signal around the molecular mass of a putative dimer, whereas protein signal at the approximate mass of a LRRK2 monomer represented a small fraction of the total. A smeared signal was also detected above the dimer size, suggesting that the LRRK2 complex includes heterologous interactors. Circumstantial evidence supporting this observation comes from two recent studies proposing that there are multiple protein interactors of LRRK2. Gloeckner *et al.* (9) showed that the chaperone Hsp90 associates with LRRK2. Similarly, Dachsel *et al.* (30) reported a large number of potential interactors for the protein when expressed in heterologous cell lines. Importantly, our results are not dependent on the use of transfected protein as similar observations were made with endogenous LRRK2.

Interestingly, we also found that kinase inactive forms of LRRK2 were mainly present in the high molecular weight complex rather than in the dimer range. However, both proteins exhibit lower steady-state expression levels when compared with wild type, which complicates the interpretation of these data. It is possible that these artificial variants may be prone to misfolding and therefore may migrate aberrantly under native conditions. Alternatively, proteins that are expressed at lower levels may be present only in heterologous complexes and therefore may be less likely to be present in the dimer. It is also plausible that phosphorylation regulates the self-interaction.

Dimer formation is observed for many protein kinases. Allosteric regulation is mediated by homodimerization in a number of serine-threonine kinases including mitogen-activated protein (MAP) kinases (31), p38, c-Jun N-terminal kinase (JNK), and their upstream kinases (32–34). We identified three potential phospho-sites in the loop, one of which, Thr-2035, is well conserved in a number of protein kinases (29) and serves as activator of kinase activity. Autophosphorylation activity of the T2035A variant was almost completely abolished as also observed previously (20), whereas decreased autophosphoryla-

tion was also detected when Ser-2032 was replaced by an alanine. We did not observe a significant change in MBP phosphorylation upon mutation of these residues when compared with the wild type. This could be consistent with either of these sites being phosphorylated, either in autophosphorylation reactions or by other kinases. However, we did not find that the addition of a negatively charged pseudophosphorylated residue convincingly increased activity. Alternatively, Ser-2032 and Thr-2035 could be important structural determinants for kinase activity, and any substitution may disrupt the conformation of the loop. Because none of these activation loop variants displayed a decreased ability to dimerize, we conclude that autophosphorylation of the activation loop *per se* is not required for dimerization. Interestingly, a truncated form of LRRK2 lacking the N-terminal region (ROC-COR-Kinase-WD40) was very active in terms of autophosphorylation, whereas proteins containing the smaller ROC-COR-kinase or only kinase domains were stable when overexpressed but completely unable to undergo autophosphorylation. These observations are in agreement with another recent report by Jaleel *et al.* (17), who found that LRRK2 activity requires an intact C terminus. This could be due to the presence of a primary autophosphorylation site in the C terminus. Alternatively, the absence of self-interaction contacts between the ROC and the WD40 domains may prevent the kinase domain from adopting the most appropriate orientation.

Although our data indicate multiple interactions among the domains, it is presently unclear whether these interactions occur in *cis*, in *trans*, or in combination. This is potentially important for the interpretation of results using pulldown assays, as performed here, to infer the mode of autophosphorylation. If the tendency of LRRK2 to form a dimer is sufficiently strong, then most of the material used in our kinase assays will presumably be dimeric, and it will therefore be difficult to distinguish between phosphorylation of adjacent monomers within each dimer *versus* each monomer phosphorylating itself. However, our data largely exclude dimer-dimer phosphorylation.

In contrast to the results reported here and those from Jaleel *et al.* (17), Luzon-Toro *et al.* (18) have shown that the LRRK2 kinase domain undergoes autophosphorylation in *trans* when expressed as a recombinant protein in *E. coli*. The reasons for the apparent discrepancy are not clear. However, the protein expressed in *E. coli* may have a different topology to the mammalian protein due to the presence of the domains outside of the kinase region as discussed above. There may also be differences in post-translational modifications that are present in mammalian cells; for example, we have shown previously that LRRK2 and the related kinase LRRK1 are basally phosphorylated when expressed in mammalian cells, for example (21). Furthermore, we have shown that LRRK2 forms dimers, but we have not found any contribution of the kinase domain to the dimer formation. It is possible that the kinase domain alone does not undergo dimerization, which might explain why the kinase domain expressed in *E. coli* shows intermolecular autophosphorylation.

In conclusion, this study shows for the first time that LRRK2, and potentially other large kinases of this class, have a complex topology that influences the kinase activity and the tendency of the protein to self-associate. We speculate that the formation of a high molecular weight complex is associated with signaling of LRRK2, a hypothesis that can be assessed when the signaling pathways of LRRK2 are elucidated.

Acknowledgments—We are very grateful to Dr. Craig Blackstone (NINDS, National Institutes of Health) for usage of the FPLC apparatus. We thank Dr. Eli Roubini of Sigma for the gift of polyclonal anti-LRRK2 antibodies.

REFERENCES

1. Paisan-Ruiz, C., Jain, S., Evans, E. W., Gilks, W. P., Simon, J., van der Brug, M., Lopez de Munain, A., Aparicio, S., Gil, A. M., Khan, N., Johnson, J., Martinez, J. R., Nicholl, D., Carrera, I. M., Pena, A. S., de Silva, R., Lees, A., Marti-Masso, J. F., Perez-Tur, J., Wood, N. W., and Singleton, A. B. (2004) *Neuron* **44,** 595–600
2. Zimprich, A., Biskup, S., Leitner, P., Lichtner, P., Farrer, M., Lincoln, S., Kachergus, J., Hulihan, M., Uitti, R. J., Calne, D. B., Stoessl, A. J., Pfeiffer, R. F., Patenge, N., Carbajal, I. C., Vieregge, P., Asmus, F., Muller-Myhsok, B., Dickson, D. W., Meitinger, T., Strom, T. M., Wszolek, Z. K., and Gasser, T. (2004) *Neuron* **44,** 601–607
3. Bras, J. M., Guerreiro, R. J., Ribeiro, M. H., Januario, C., Morgadinho, A., Oliveira, C. R., Cunha, L., Hardy, J., and Singleton, A. (2005) *Movement Disorders* **20,** 1653–1655
4. Ozelius, L. J., Senthil, G., Saunders-Pullman, R., Ohmann, E., Deligtisch, A., Tagliati, M., Hunt, A. L., Klein, C., Henick, B., Hailpern, S. M., Lipton, R. B., Soto-Valencia, J., Risch, N., and Bressman, S. B. (2006) *N. Engl. J. Med.* **354,** 424–425
5. Lesage, S., Durr, A., Tazir, M., Lohmann, E., Leutenegger, A. L., Janin, S., Pollak, P., and Brice, A. (2006) *N. Engl. J. Med.* **354,** 422–423
6. Bonifati, V. (2007) *Neurochem. Res.* **32,** 1700–1708
7. Whaley, N. R., Uitti, R. J., Dickson, D. W., Farrer, M. J., and Wszolek, Z. K. (2006) *J. Neural Transm. Suppl.* **70,** 221–229
8. Funayama, M., Hasegawa, K., Kowa, H., Saito, M., Tsuji, S., and Obata, F. (2002) *Ann. Neurol.* **51,** 296–301
9. Gloeckner, C. J., Kinkl, N., Schumacher, A., Braun, R. J., O'Neill, E., Meitinger, T., Kolch, W., Prokisch, H., and Ueffing, M. (2006) *Hum. Mol. Genet.* **15,** 223–232
10. Greggio, E., Jain, S., Kingsbury, A., Bandopadhyay, R., Lewis, P., Kaganovich, A., van der Brug, M. P., Beilina, A., Blackinton, J., Thomas, K. J., Ahmad, R., Miller, D. W., Kesavapany, S., Singleton, A., Lees, A., Harvey, R. J., Harvey, K., and Cookson, M. R. (2006) *Neurobiol. Dis.* **23,** 329–341
11. Guo, L., Gandhi, P. N., Wang, W., Petersen, R. B., Wilson-Delfosse, A. L., and Chen, S. G. (2007) *Exp. Cell Res.* **313,** 3658–3670
12. Lewis, P. A., Greggio, E., Beilina, A., Jain, S., Baker, A., and Cookson, M. R. (2007) *Biochem. Biophys. Res. Commun.* **357,** 668–671
13. Li, X., Tan, Y. C., Poulose, S., Olanow, C. W., Huang, X. Y., and Yue, Z. (2007) *J. Neurochem.* **103,** 38–47
14. West, A. B., Moore, D. J., Biskup, S., Bugayenko, A., Smith, W. W., Ross, C. A., Dawson, V. L., and Dawson, T. M. (2005) *Proc. Natl. Acad. Sci. U. S. A.* **102,** 16842–16847
15. Funayama, M., Hasegawa, K., Ohta, E., Kawashima, N., Komiyama, M., Kowa, H., Tsuji, S., and Obata, F. (2005) *Ann. Neurol.* **57,** 918–921
16. Smith, W. W., Pei, Z., Jiang, H., Dawson, V. L., Dawson, T. M., and Ross, C. A. (2006) *Nat. Neurosci.* **9,** 1231–1233
17. Jaleel, M., Nichols, R. J., Deak, M., Campbell, D. G., Gillardon, F., Knebel, A., and Alessi, D. R. (2007) *Biochem. J.* **405,** 307–317
18. Luzon-Toro, B., de la Torre, E. R., Delgado, A., Perez-Tur, J., and Hilfiker, S. (2007) *Hum. Mol. Genet* **16,** 2031–2039
19. West, A. B., Moore, D. J., Choi, C., Andrabi, S. A., Li, X., Dikeman, D., Biskup, S., Zhang, Z., Lim, K. L., Dawson, V. L., and Dawson, T. M. (2007) *Hum. Mol. Genet* **16,** 223–232
20. Ito, G., Okai, T., Fujino, G., Takeda, K., Ichijo, H., Katada, T., and Iwatsubo, T. (2007) *Biochemistry* **46,** 1380–1388
21. Greggio, E., Lewis, P. A., van der Brug, M. P., Ahmad, R., Kaganovich, A.,

Ding, J., Beilina, A., Baker, A. K., and Cookson, M. R. (2007) *J. Neurochem.* **102,** 93–102
22. Korr, D., Toschi, L., Donner, P., Pohlenz, H. D., Kreft, B., and Weiss, B. (2006) *Cell. Signal.* **18,** 910–920
23. Melrose, H. L., Kent, C. B., Taylor, J. P., Dachsel, J. C., Hinkle, K. M., Lincoln, S. J., Mok, S. S., Culvenor, J. G., Masters, C. L., Tyndall, G. M., Bass, D. I., Ahmed, Z., Andorfer, C. A., Ross, O. A., Wszolek, Z. K., Delldonne, A., Dickson, D. W., and Farrer, M. J. (2007) *Neuroscience* **147,** 1047–1058
24. Zhou, H., and Zhou, Y. (2005) *Proteins* **61,** Suppl. 7, 152–156
25. Thompson, J. D., Gibson, T. J., Plewniak, F., Jeanmougin, F., and Higgins, D. G. (1997) *Nucleic Acids Res.* **25,** 4876–4882
26. Xiang, Z., Soto, C. S., and Honig, B. (2002) *Proc. Natl. Acad. Sci. U. S. A.* **99,** 7432–7437
27. Shi, Z., Resing, K. A., and Ahn, N. G. (2006) *Curr. Opin. Struct. Biol.* **16,** 686–692
28. Deng, J., Lewis, P. A., Greggio, E., Sluch, E., Beilina, A., and Cookson, M. R. (2008) *Proc. Natl. Acad. Sci. U. S. A.* **105,** 1499–1504
29. Nolen, B., Taylor, S., and Ghosh, G. (2004) *Mol. Cell* **15,** 661–675
30. Dachsel, J. C., Taylor, J. P., Mok, S. S., Ross, O. A., Hinkle, K. M., Bailey, R. M., Hines, J. H., Szutu, J., Madden, B., Petrucelli, L., and Farrer, M. J. (2007) *Parkinsonism Relat. Disord.* **13,** 382–385
31. Ohren, J. F., Chen, H., Pavlovsky, A., Whitehead, C., Zhang, E., Kuffa, P., Yan, C., McConnell, P., Spessard, C., Banotai, C., Mueller, W. T., Delaney, A., Omer, C., Sebolt-Leopold, J., Dudley, D. T., Leung, I. K., Flamme, C., Warmus, J., Kaufman, M., Barrett, S., Tecle, H., and Hasemann, C. A. (2004) *Nat. Struct. Mol. Biol.* **11,** 1192–1197
32. Song, J. J., and Lee, Y. J. (2003) *J. Biol. Chem.* **278,** 47245–47252
33. Cheng, J., Yu, L., Zhang, D., Huang, Q., Spencer, D., and Su, B. (2005) *J. Biol. Chem.* **280,** 13477–13482
34. Leung, I. W., and Lassam, N. (2001) *J. Biol. Chem.* **276,** 1961–1967